# Lab Call FY18 (Reversible Fuel Cell): Technology-Enabling Materials, Cell Design for Reversible Proton Exchange Membrane Fuel Cells

Nemanja Danilovic (Primary Contact), Deborah Myers (ANL), Yagya Regmi
Lawrence Berkeley National Laboratory (LBNL)
1 Cyclotron Rd, 30-124
Berkeley, CA 94720
Phone: 510-486-7045
Email: ndanilovic@lbl.gov

DOE Manager: Gregory Kleen
Phone: 240-562-1672
Email: Gregory.Kleen@ee.doe.gov

Subcontractor:
Argonne National Laboratory (ANL), Argonne, IL

Project Start Date: January 1, 2018
Project End Date: December 31, 2019

## Overall Objectives

The objective of the project is to demonstrate feasibility of a unitized regenerative fuel cell (URFC) configuration that has the potential to be higher performing and more stable that the URFCs that have been tested and reported to date. Specifically:

- Show feasibility of the proton exchange membrane (PEM) URFC at the 5–25 $cm^2$ level that operates in a constant electrode configuration and conventional catalysts.
- Compare constant gas and constant electrode modes of URFC operation.
- Show feasibility of the proposed thin films of platinum group metal (PGM) catalysts on non-carbon supports using rotating disk electrode (RDE) screening studies and in membrane electrode assembly (MEA) testing.

## Fiscal Year (FY) 2019 Objectives

- Demonstrate cycling performance under different URFC modes.
- Determine optimal Pt/Ir ratio or structure using atomic layer deposition (ALD).
- Demonstrate scalability of the ALD process.
- Translate ALD-synthesized URFC catalysts into an MEA.
- Demonstrate discrete performance of URFC MEA containing down-selected thin film anode catalyst in fuel cell and electrolyzer modes within 100 mV of baseline fuel cell (Pt/C) and electrolyzer ($IrO_2$ black) MEAs in their respective modes of operation at 1 $A/cm^2$.

## Technical Barriers

This project addresses the following technical barriers from the Fuel Cells and Hydrogen Production sections of the Fuel Cell Technologies Office Multi-Year Research, Development, and Demonstration Plan[1]:

- Fuel Cells—Catalyst, catalyst support, and membrane electrode assembly:
  - A: Durability
  - B: Cost
  - C: Performance.
- Hydrogen Production—Catalyst, catalyst support, and membrane electrode assembly:
  - F: Capital cost
  - G: System efficiency and electricity cost.

## Technical Targets

The DOE technical targets and our current project status are listed in Table 1 for comparison.

This project evaluates different modes of URFC operation and evaluates supported and unsupported bifunctional catalysts:

- Cost: capital cost reduction through reduction in catalyst loading and membrane thickness
- Efficiency improvement: through optimized operating conditions and modes.

[1] https://www.energy.gov/eere/fuelcells/downloads/fuel-cell-technologies-office-multi-year-research-development-and-22

## FY 2019 Accomplishments

- Pt and Ir deposited by ALD onto $TiO_2$ met our ex situ RDE performance target:
  - Total metal loading on $TiO_2$ is ~24 wt % in optimal 90-10 Ir-Pt ratio.
  - Ir-Pt_90-10@$TiO_2$ has higher mass activity than Pt black and Pt@C.
  - Compared to commercial Ir black, Ir-Pt_90-10@$TiO_2$ has 46 mV higher overpotential at 100 mA/mg-Ir.
  - Scale up of catalyst was achieved for MEA translation.
- The down-selected 90 at % Ir-10 at % Pt catalyst layer, consisting of commercial unsupported catalysts in a complete URFC, demonstrated round-trip efficiency approaching 60% at a total PGM loading of 1.3 mg/cm$^2$ in fixed electrode mode. Fixed electrode mode outperforms fixed gas mode.
- Durability evaluation by accelerated stress test (AST) showed good stability in the target range of ~5,000 cycles
- Accomplishment. APR Front Bullet. APR Front Bullet. APR Front Bullet. APR Front Bullet. APR Front Bullet.

**Table 1. Project Technical Targets**

| Specification | Baseline Fuel Cell | Baseline Electrolyzer | Baseline URFC | Proposed URFC | Achieved to Date |
|---|---|---|---|---|---|
| Membrane thickness (microns) | 25 | 125 | 125–175 | 50–60 | 50 |
| Total cell Pt catalyst loading (mg/cm$^2$) | 0.4 | 1 | 6 | 0.8 | 0.4 |
| Ir catalyst loading (mg/cm$^2$) | n/a | 2 | 4 | 1 | 0.9 |
| Fuel cell stack efficiency | >50% | n/a | <40% | >50% | 58% |
| Electrolysis stack efficiency | n/a | ~65% | <55% | >75% | 99% |
| Round-trip electrical efficiency | n/a | n/a | <25% | >45% | 57% |

## INTRODUCTION

As described in the DOE H2@Scale initiative, a promising means to store large amounts of energy at low cost is to utilize electrolysis to produce hydrogen and a fuel cell to convert that hydrogen back to electricity as needed. If the electrolyzer and fuel cell are separate devices, the system is termed a discrete reversible or regenerative fuel cell; the combination of the two processes in one device is termed a unitized reversible or regenerative fuel cell. In principle, a URFC should decrease catalyst, membrane, and balance of cell and plant costs relative to a discrete system that requires twice the materials. The primary barriers to widespread implementation of the traditional URFC device are high cost, low efficiency, and limited lifetime. We address these barriers in the work below.

## APPROACH

To overcome the above-mentioned electrocatalytic, stability, and transport issues with the traditional URFC design, LBNL and ANL propose an alternative cell design that enables an improved electrode layer and novel catalysts that decrease precious metal loadings. We combine oxygen evolution (OER) and hydrogen oxidation (HOR) reactions on one electrode (the anode) and hydrogen evolution (HER) and oxygen reduction (ORR) reactions on the other electrode (the cathode), as shown in Figure 1, in what we call constant electrode mode. This novel cell design allows optimization of the catalysts and electrode wetting for the two URFC reactions, OER and ORR, responsible for the majority of the efficiency loss and cost in the traditional design.

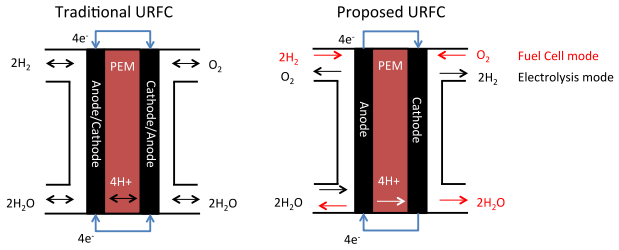


**Figure 1. URFC operating modes: traditional (constant gas) vs. proposed (constant electrode)**

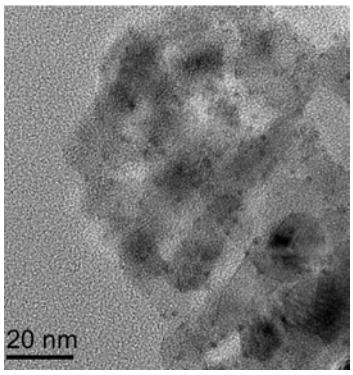


Figure 2. Representative transmission electron microscopy (TEM) micrograph of 90_10-Ir_Pt@TiO2 (40 nm), showing 1–2 nm particles of Pt and Ir on the support

## RESULTS

### Supported Catalyst Development

Ir and Pt were deposited on titania supports of two sizes, 5 nm and 40 nm support primary particle size, as well as a titanium nitride support and a titanium carbide support. The target Pt to Ir ratio was 50%; however, it was determined by inductively-coupled plasma–optical emission spectrometry (ICP-OES) that the atomic ratio of Pt to Ir in these samples was 73:27. The Ir and Pt were deposited by alternating deposition cycles of Ir and Pt. The X-ray diffraction (XRD) patterns of these materials indicated that an alloy of Pt and Ir was formed. These materials were highly active for HOR but showed higher than desired OER overpotentials. The next cycle used a higher Ir content and lower Pt content with targeted Ir to Pt atomic ratios of 90:10 and 95:5, aiming to match the Pt/Ir black baseline ratio from MEA tests. The depositions were only performed on the titania supports because those resulted in the most active catalyst in FY 2018 Q4 testing. The deposition procedure was altered such that all the Ir was deposited first followed by deposition of Pt. The rationale behind this was to maximize the electrochemically-active surface area of Pt. It has also been shown, by 3M, that an Ir underlayer on their nanostructured thin film-supported catalysts improves the durability of a Pt overlayer. The XRD patterns of the new samples showed that there was no or undetectable alloying of Ir with Pt; however, the XRD peaks were very broad, presumably due to small crystallite size. Analysis of these four samples by ICP-OES showed that the Ir to Pt ratio was lower than the target ratios of 90:10 and 95:5 (actual values: 65–70 at % Ir and 87–88 at % Ir). TEM characterization of the samples prepared in FY 2018 and FY 2019 showed that nanoparticles of 0.5 to 4.5 nm were formed (Figure 2), rather than the target thin film morphology, and that the deposition was not uniform across all support particles/aggregates.

All $TiO_2$-supported catalysts tested showed high HOR activity, with <10 mV higher HOR overpotential at 2 $mA/cm^2$-geo current density versus the Tanaka Pt black and Umicore Pt/HSC reference (Figure 3). The OER activity tests of the $TiO_2$-supported catalyst and of the Ir standards, with comparable Ir loadings on the RDE tip, showed that the $TiO_2$-supported catalysts have both higher kinetic overpotentials for OER and higher mass-transport overpotentials through the relatively thicker catalyst films versus those of the unsupported Ir-Black and commercial $IrO_2$. In other words, the low metal loading on supports required more supported catalyst to be deposited onto the RDE tip to match the total metal loading. We note that this is an artifact of the RDE measurement specifically and is a net benefit in fabricating thicker, more uniform catalyst layers for MEA testing. Due to these transport-related limitations, the overpotentials were compared at 5 $mA/cm^2$-geo rather than the milestone target of 10 $mA/cm^2$-geo. The Ir-Pt 90:10 on 40 nm $TiO_2$ had the highest OER activity with an OER overpotential at 5 $mA/cm^2$ that was 88 mV higher than the commercial $IrO_2$ standard (Figure 3). When normalized to the mass of Ir on the electrode, the $TiO_2$-supported catalysts showed OER overpotentials 38 to 94 mV higher than that of the $IrO_2$-black reference at 100 mA/mg-Ir and 200 mA/mg-Ir.

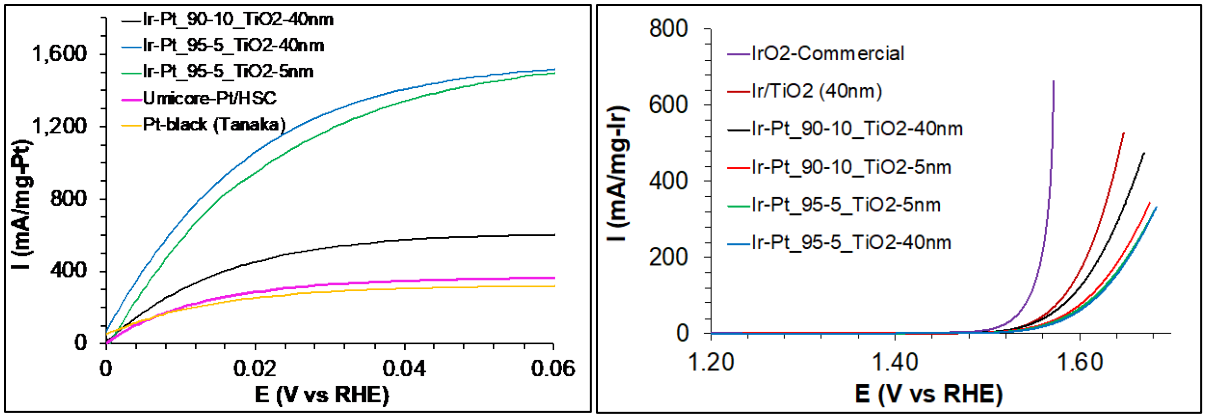


Figure 3. HOR and OER performance data at beginning of life for baseline commercial materials and ANL-produced supported catalysts

Thus, the Ir-Pt 90:10 on 40 nm $TiO_2$ simultaneously meets both our HOR and OER activity targets compared to baseline catalysts at 5 mA/cm$^2$, remarkably with a total metal loading of 13 wt % (Pt+Ir) on $TiO_2$.

Next, durability testing was performed on the Ir-Pt 90:10/$TiO_2$_40 nm sample. Two loadings of the catalyst on the RDE tip were tested: 20 µg-Ir/cm$^2$ and 40 µg-Ir/cm$^2$. The catalyst was cycled in deaerated 0.1 M $HClO_4$ from 0.05 V to 1.6 V at a scan rate of 50 mV/s. This range was chosen to be representative of the voltages that would be experienced by the URFC anode during transitions between fuel cell and electrolysis modes. As shown in Figure 4, after 2,000 cycles, the OER overpotential at 2 mA/cm$^2$-geo of the 40 µg-Ir/cm$^2$ deposit increased by 48 mV after 4,000 cycles. After 5,000 cycles, the 20 µg-Ir/cm$^2$ deposit did not reach 2 mA/cm$^2$ at 1.7 V. The 20 µg-Ir/cm$^2$ deposit showed almost complete loss of HOR activity after 5,000 cycles (HOR activity during cycling was not monitored). It should be noted that both deposits showed a decrease in OER overpotential after 100 cycles. Based on the loss of HOR activity with cycling, the initial improvement in OER activity with cycling may arise from the loss of Pt and the concomitant increase in the electrochemically-active surface area of the Ir.

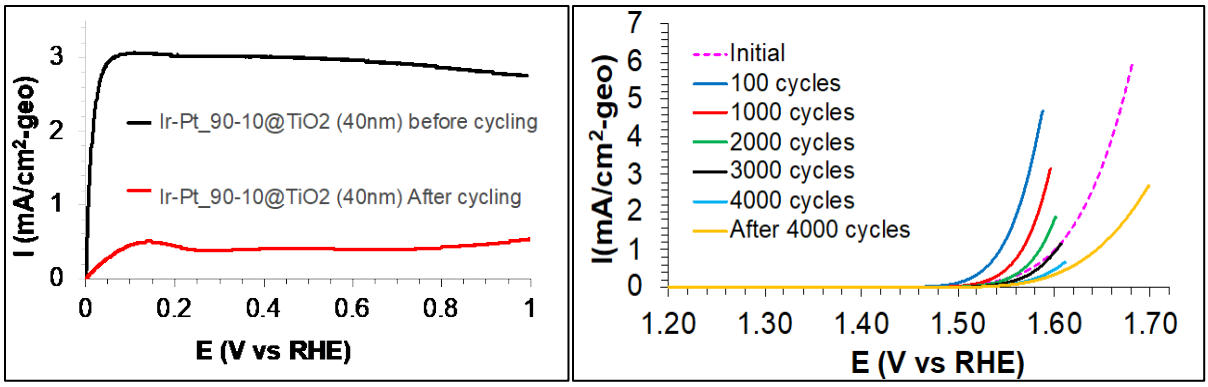


Figure 1. HOR and OER durability data for ANL-produced supported catalysts

Thus, the Ir-Pt 90:10 on 40 nm $TiO_2$ does meets our OER durability target (at 2 mA/cm$^2$) up to 2,000 h of AST cycles, which represents 5 years' worth of 12-h URFC duty cycles. However, without optimization, the 5,000 cycle target was not achieved.

### URFC Optimization

The optimized composition of the anode catalyst layer was studied using commercial unsupported materials from TKK. We refined our MEA fabrication and cell testing and assembly for and tested the URFC MEA in a URFC cell; data are shown in Figure 5. This test consisted of an MEA that was prepared with the URFC catalyst composition and deposited onto N212. The cell hardware had the parallel channel flowfield optimized

for electrolyzer operation, and we applied a hydrophobic treatment on the Ti porous transport layer. The catalyst composition using commercial Pt and Ir black had previously been down-selected to 10/90 at % ratio, respectively.

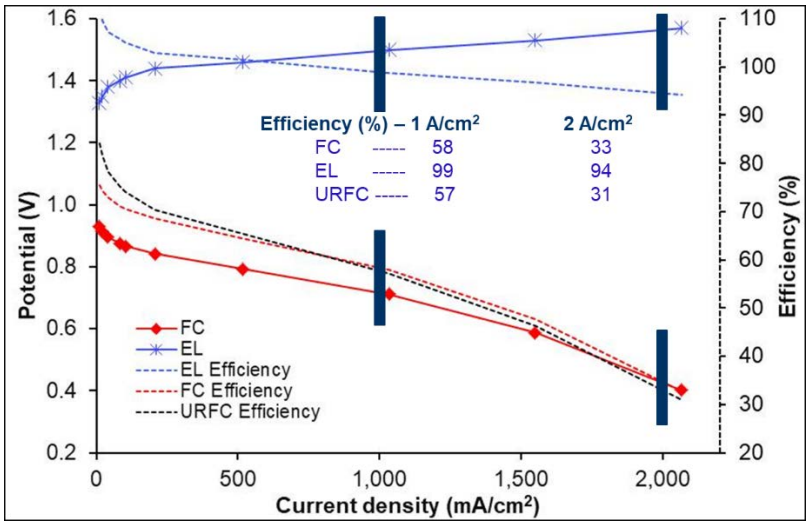


Figure 2. Polarization curves for 5-cm² URFC MEA in unitized cell hardware and components: N212-boiled membrane, with 29BC gas diffusion layer on the cathode and teflonized porous Ti-PTL on the anode. The round-trip efficiency was 57% at 1 A/cm².

### Accelerated Stress Tests and Durability

The optimized URFC MEA in the URFC cell with parallel channel flowfield on the HOR/OER (anode) side was used for AST. The test consisted of a fuel cell break-in followed by fuel cell and electrolyzer performance testing. The fuel cell test first was found to result in better fuel cell performance then when the cell was operated as an electrolyzer first. The anode side was then cycled potentiostatically between 0.05 V and 1.65 V (1 A/cm$^2$ in electrolysis mode) for n number of cycles up to 10,000 with liquid water flowing on the anode during the AST. Periodically the test was stopped in order to test the electrolyzer and fuel cell performance. Figure 6 (left) shows the summary of the AST, with the relative performance change denoting the fraction of performance at n cycles relative to cycle 0 (i.e., electrolyzer: @ 1 A/cm$^2$ Vcell @ n cycle / Vcell @ 0; fuel cell: @ 0.55 V Vcell @ n-cycle / Vcell @ 0). The round-trip efficiency is also plotted as a function of cycles.

Round-trip efficiency is calculated by the following formulas, at 1 A/cm$^2$ in respective mode of operation:

**Efficiency Calculations for FC**

$$\frac{\textit{Operating voltage at 1A per cm}^2}{\textit{Thermodynamic voltage (1.229)}} \times 100$$

**Efficiency Calculations for EL**

$$\frac{\textit{Thermal neutral voltage (1.481)}}{\textit{Cell operating voltage at 1 A per cm}^2} \times 100$$

**Efficiency URFC**

FC x EL

The degradation is limited to fuel cell mode; after an initial improvement in performance, the performance degrades. The overall reduction in round-trip efficiency is from 55% to 45%. The gap is due to this test being performed over the course of 24 h; it was timed so that the beginning and end point performance tests could be obtained during work hours.

We also performed a durability test using the duck curve problem as a scenario for testing. In the duck curve scenario, there is excess electricity for about 6 h during the day when there is substantial solar energy on the grid, followed by 4 h of an electrical rut where there is a lack of electricity due to a lack of solar at night. Thus, an energy conversion device is required to shift the available power from the times of excess to the times of need. We evaluated this over the course of 3 days in which we charged the URFC for 6 h at constant 1 A/cm$^2$, followed by a 4 h discharge at 1 A/cm$^2$. The results shown in Figure 6 (right) indicate that, similar to the AST

cycles performed, the electrolyzer (charge mode) remains durable over the timeframe, but the fuel cell (discharge) mode degrades from day to day. Note no degradation is observed during the steady holds.

Thus, similar to the RDE AST and durability results, the fuel cell mode or HOR suffers the most degradation during testing. Presumably due to Pt loss, agglomeration, or migration, there is a significant detriment to the fuel cell mode of operation. Our future work will focus on the degradation mechanisms and the discrepancy between AST and durability testing.

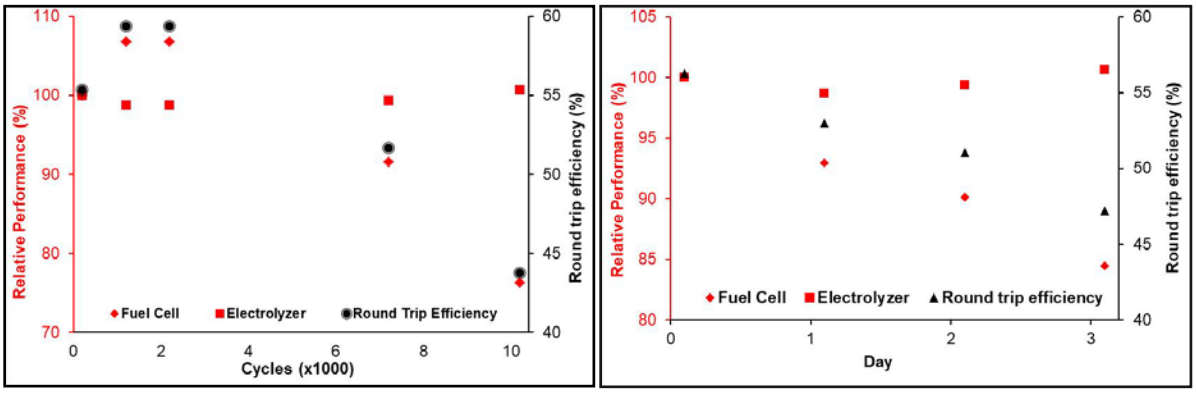


Figure 3. AST in constant electrode mode (HOR/OER, bifunctional electrode) over 10,000 cycles (left); and durability cycling under constant electrode conditions, cycles consisted of 6 h electrolyzer and 4 h fuel cell holds at 1 A/cm², following a duck curve profile (right).

## CONCLUSIONS AND UPCOMING ACTIVITIES

In conclusion, constant electrode URFC operation is favorable compared to constant gas operation; we demonstrated 57% round-trip efficiency of a fully URFC MEA and cell. The approach of using ALD to prepare supported catalysts was also validated by obtaining good HOR and OER bifunctional electrocatalysts under RDE conditions. ASTs performed both in RDE and MEA show that fuel cell operation degrades with AST cycles, while electrolyzer performance can be maintained. The reasons for degradation are being investigated.

Remaining work prior to the end of the project includes:

1. Integrate ANL-supported catalysts into URFC MEA and evaluate performance and AST.
2. Tune AST procedure to be comparable with durability test.
3. Determine cause of degradation.

## FY 2019 PUBLICATIONS/PRESENTATIONS

1. Yagya Narayan Regmi, Julie Fornaciari, Max Wei, Debbie Myers, Adam Z. Weber, and Nemanja Danilovic, “Experimental Analysis of Operating Conditions of Proton Exchange Membrane Based Unitized Regenerative Fuel Cells for Efficient and Economic Energy Conversion,” Meeting of the Electrochemical Society, Dallas, TX, May 1, 2019.